Polymer Communication

Influence of strain rate, temperature and humidity on the tensile yield behaviour of aliphatic polyketone

L.E. Govaert[a,*], P.J. de Vries[a], P.J. Fennis[b], W.F. Nijenhuis[b], J.P. Keustermans[b]

[a]*Dutch Polymer Institute (DPI), Materials Technology (MaTe), Eindhoven University of Technology, P.O. Box 513, 5600 MB Eindhoven, The Netherlands*
[b]*Shell Research and Technology Centre, Amsterdam, The Netherlands*

Abstract

The tensile yield behaviour of an aliphatic polyketone is studied in relation to the molecular relaxation processes present in the polymer. Dynamic mechanical thermal analysis reveals the presence of three molecular relaxation mechanisms; the crystalline α-, and the amorphous β- and, γ-process. The tensile yield behaviour, measured over a large range of temperature and strain rate, also gives evidence of these three relaxation mechanisms. The increase of the water content from 0.5 to 2.3 wt% leads to a selective change in the β-contribution, whereas the α- and γ-processes show little to no change. With respect to the tensile yield behaviour this leads to a reduction of the yield stress at high strain rates and/or low temperatures. © 1999 Elsevier Science Ltd. All rights reserved.

Keywords: Aliphatic polyketone; Tensile behaviour; Yield

1. Introduction

The copolymerisation of carbon monoxide into α-olefin based polymers has been of considerable interest to the chemical industry. This interest was motivated by the abundance of the raw materials, as well as by the envisioned influence on the thermal properties of the polymer. However, although copolymers of ethylene and carbon monoxide of formula $-(-CH_2-CH_2-CO)_n-$ were synthesised in the past [1–3], it is only since the work of Drent et al. [4,5] that it has become technologically feasible to produce perfectly alternating copolymers. Recently, these semi-crystalline aliphatic polyketones have been introduced by Shell under the trademark CARILON. The first type that is being commercialised, (CARILON EP polymer, which is the specific type under investigation in this work) is a terpolymer of carbon monoxide, ethylene and a few percent of propylene polymerised into a linear, perfectly alternating olefin/CO structure. This terpolymer exhibits many desirable characteristics like a high resilience, good chemical resistance and superior barrier performance to hydrocarbons and small gases such as oxygen [6–8].

In the present investigation the deformation behaviour of CARILON EP polymer is studied using dynamic mechanical thermal analysis (DMTA) and uni-axial tensile experiments. The study focuses on the influence of temperature, strain rate and moisture. The results are discussed in an attempt to relate the observed behaviour to events occurring on a molecular scale.

2. Experimental

2.1. Materials

The aliphatic polyketone used in this study is CARILON EP polymer of DP P1000 grade, a terpolymer of 50 mol% carbon monoxide, about 44 mol% ethylene and approximately 6 mol% of propylene. The glass transition temperature, T_g and the melting point, T_m of the DP P1000 grade are approximately 15 and 220°C, respectively [6].

2.2. Preconditioning

Two different methods were applied to precondition the test specimen. One part of the samples, further referred to as 'dry', was conditioned for at least 1 week at 20°C and 60% relative humidity (RH), resulting in a water content of 0.5 wt%. The other part of the samples, further referred to as 'wet', was stored for at least two weeks at 20°C in water, resulting in a water content of 2.3 wt%.

2.3. Techniques

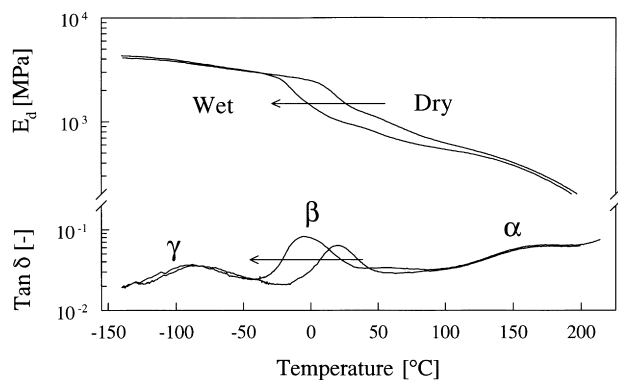Dynamic mechanical thermal analysis was performed on

---

* Corresponding author.

Fig. 1. Temperature dependence of the dynamic modulus E_d and the loss factor tan δ for aliphatic polyketone (CARILON polymer of DP P1000 grade). The arrow indicates the effect of an increase of water content from 0.5 to 2.3 wt%.

a DMTA MkIII, from Rheometrics Scientific. Temperature scans at a heating rate of 2°C/min were performed in uni-axial extension at a frequency of 1 Hz, using rectangular-shaped specimen $(25 \times 4 \times 1 \text{ mm}^2)$. Tensile tests were performed on injection molded dumbbell specimen (ASTM 638 DIII), using a Zwick Rel servo-hydraulic tensile tester equipped with a thermostatically controlled oven and extensometers (both longitudinal and transversal). Tensile tests were performed at strain rates ranging from 5×10^{-4} to 12 s^{-1} and temperatures from -50 to 75°C.

3. Results and discussion

3.1. Dynamic mechanical thermal analysis

In Fig. 1 the temperature dependence of the dynamic modulus E_d and the loss factor tan δ are presented for both 'dry' and 'wet' samples. In both cases the shape of the tan δ curve clearly reveals three different transitions, labelled α, β and γ in order of decreasing temperature. This behaviour can qualitatively be compared to that of
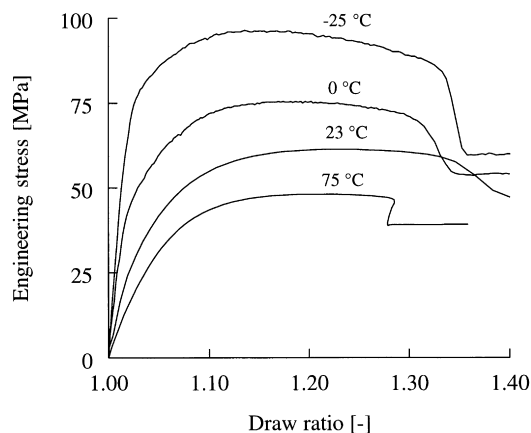

Fig. 2. Engineering stress versus draw ratio at various temperatures in uniaxial extension at a strain rate of 0.05 s^{-1}.

other highly crystalline polymers like for instance PE (Poly-ethylene), PP (Polypropylene), PA (Polyamide) or POM (Polyoxymethylene), which also display three different molecular relaxation mechanisms [9–11]. In these materi-als, the high-temperature transition α is always attributed to processes within the crystalline fraction [9–11]. More speci-fically, it is regarded to originate from chain transport as a result of the diffusion of defects throughout the crystalline material. The lower temperature transition β, is the glass transition, attributed to the amorphous material and related to main-chain segmental motion. The γ-process, in Fig. 1 located at approximately -80°C, could be related to side-chain motion, e.g. a secondary glass transition (T_γ), of the amorphous material. Generally, the low temperature γ-process in semi-crystalline polymers is agreed to have at least in part amorphous phase origin [9].

The effect of an increase in the water content is visible as a shift in the glass transition temperature, indicated with an arrow in Fig. 1, and as an increase in tan δ peak height (this proves that the β-transition reflects T_g). This increase of the peak height is in agreement with the observed decrease in the relaxed dynamic modulus (E_d) of the β-process and hence the increased relaxation strength. It is evident that water is an effective plasticizer that makes it easier for changes in molecular conformation to occur, and so lower the glass transition temperature.

3.2. Tensile behaviour

Fig. 2 shows the engineering stress versus draw ratio as measured in uniaxial extension (strain rate of 0.05 s^{-1}) for several temperatures. As to be expected, it is observed that the overall stress level increases with decreasing tempera-ture. The experimental results, presented in Fig. 2, clearly reflects the presence of the glass transition (β) at a tempera-ture of 15°C. Firstly there is a strong increase of the modulus with decreasing temperature (750 MPa at 75°C, 3700 MPa at -25°C), indicating that the amorphous phase has trans-formed to the glassy state. Secondly, with decreasing temperature a sharp 'bend' appears in the tensile response at a relatively low strain of approximately 3%. This 'bend' indicates the onset of yield in the glassy amorphous phase. In the rubbery state the amorphous phase will not give rise to yield phenomena (unless loaded at high strain rates as will be elaborated further on) and therefore the 'bend' in the curve disappears simultaneously with a strong decrease of the modulus.

Unlike the distinct yield point for the amorphous phase, the onset of yield in the crystalline phase is less clear. The maximum in the engineering stress is found at approxi-mately 15–20% strain, whereas necking typically occurs at much higher strain levels (25–35%). The strain to break ranges 300–350%. The rather high strain level at which necking occurs is remarkable, as a deformation stage of decreasing engineering stress with increasing strain is very unstable and usually triggers necking much faster.
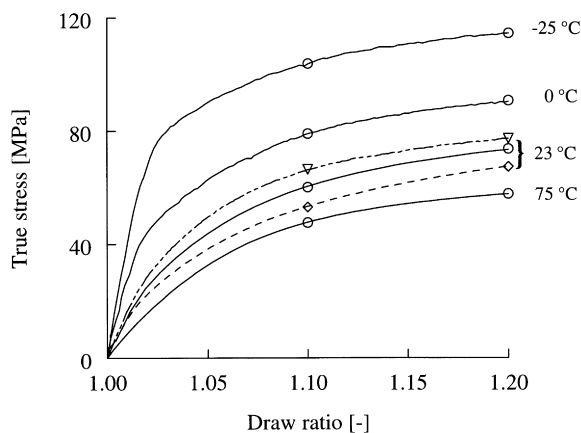
Fig. 3. True stress versus draw ratio at various temperatures. The applied strain rates were 4×10^{-4} s^{-1} ($\diamond$), 5×10^{-2} s^{-1} ($\bigcirc$) and 2.1 s^{-1} ($\triangle$).

On the other hand, however, the unstable character of the deformation is this stage was reflected in a rather strong variation of the strain level at which necking occurred.

Fig. 3 shows true stress versus draw ratio of the curves presented in Fig. 2, as well as a few additional curves at different strain rates. The curves are only considered up to a draw ratio of 1.2 (20% strain), to avoid influence of the unstable deformation that occurs after the maximum in the engineering stress. In the range of strains considered, no maximum in the true stress is observed. On the other hand, it is observed that, at strain levels exceeding 5%, the tensile responses at different temperatures and strain rates are approximately parallel, indicating that the change in stress level as a function of strain rate and/or temperature is the same for draw ratios ranging about 1.1 and up. In other words, for large strains an increase in strain rate or a decrease in temperature results in an increase of the stress level with a constant factor. In the absence of a clearly defined yield stress, the further analysis of the yield behaviour was therefore based on the stress level at a constant
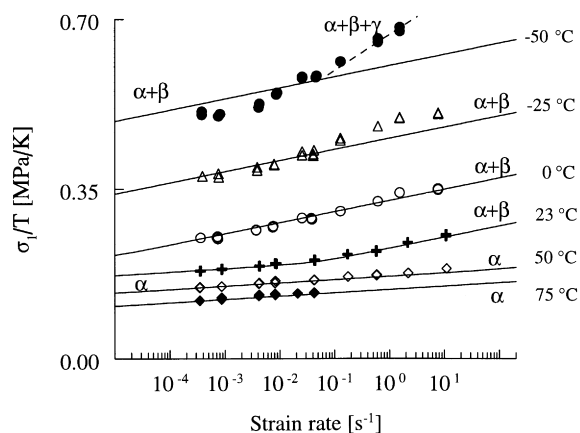

Fig. 4. Strain rate dependence of the 10%-stress σ_1 at various temperatures. The solid lines are fits, obtained using Eq. (1) and the parameters is given in Table 1.

draw ratio of 1.10 (10% strain), further referred to as the 10%-stress σ_1.

The strain rate dependence of the 10%-stress σ_1 at various temperatures is presented in Fig. 4. Similar to the yield behaviour of isotactic Polypropylene [12] (i-PP), Polycarbonate [13] (PC), Polymethylmethacrylate [14] (PMMA), Polyethylmethacrylate [15] (PEMA) and Poly-vinylchloride [16] (PVC), it appears that the aliphatic poly-ketone considered in this study displays the specific contributions from at least two molecular processes, the crystalline α- and the amorphous β-process. At low strain rate and/or high temperatures, the deformation is governed by a single process: the α-transition. With increasing strain rate and decreasing temperature, however, the β-process starts to contribute to the stress level, as indicated schematically in Fig. 4. The most important result of this stress contribution is that the yield stress will increase much faster as a function of strain rate witnessed by an increase of the slope of the curve.

The experimental results at $-50°C$ give evidence of a further increase of the slope of the curve, which is indicative for the onset of a contribution of the γ-process. Especially at low temperature this will have a considerable influence on the yield behaviour at high deformation rates. However, as there is only limited data available on the γ-contribution (which is only visible at $-50°C$), it is omitted in the following and the data was further analysed in terms of two stress (and temperature) activated processes. In this case the strain rate dependence of the 10%-stress σ_1 is modelled in terms of two separate contributions acting in parallel [11–17], where each contribution is described by an Eyring equation:

$$\frac{\sigma}{T} = \frac{k}{v_\alpha} \sinh^{-1} \left[\frac{\dot{\varepsilon}}{C_{0,\alpha}} \exp\left(\frac{\Delta H_\alpha}{RT} \right) \right]$$
$$+ \frac{k}{v_\beta} \sinh^{-1} \left[\frac{\dot{\varepsilon}}{C_{0,\beta}} \exp\left(\frac{\Delta H_\beta}{RT} \right) \right] \tag{1}$$

where k is Boltzmanns constant, R the gas constant, v_α and v_β the activation volumes, ΔH_α and ΔH_β the activation energies and $C_{0,\alpha}$ and $C_{0,\beta}$ the pre-exponential factors of the α- and β-process, respectively. The solid lines in Fig. 4 are predictions using Eq. (1) and the parameters listed in Table 1. It is clear that an accurate description is obtained over a large range of temperature and strain rate.

The results of Fig. 4 seem to be in good agreement with the observations in Fig. 1. At relatively high temperature and low strain rate the deformation behaviour is dominated by the crystalline α-relaxation process. The α-process is therefore the predominant mechanism in long-term loading situations, like creep. At specific lower temperatures and/or higher strain rates, the time-scale of the mechanical measurement will reach the order of the time-scale of one of the other molecular relaxation processes. Then, the other processes that become involved in the deformation will start to contribute to the total stress observed in tensile
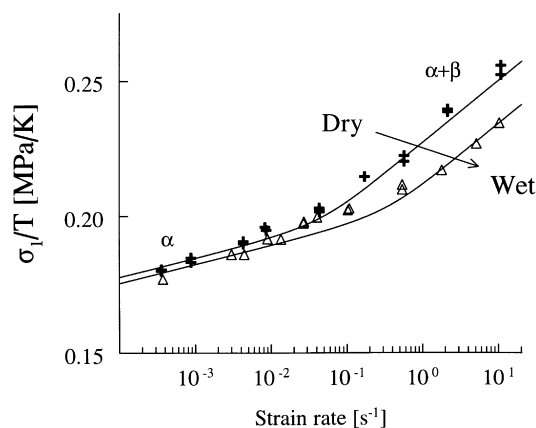
Fig. 5. Strain rate dependence of the 10% stress σ_1 at 23°C for 'wet' and 'dry' samples. The solid lines represent predictions using Eq. (1) and the parameters in Table 1. In the case of the 'wet' samples $C_{0,\alpha} = 10^{33}$ and $C_{0,\beta} = 10^{46}$ s^{-1}.

experiments [12–17]. The secondary β- and possibly even the tertiary γ-relaxation process, therefore, are of particular importance in the short-term mechanical behaviour.

In Fig. 5 the influence of the water content on the strain rate dependence of the 10% stress σ_1 at room temperature is presented. It is clear that an increase in water content reduces the yield stress over the entire range experimentally covered. However, at high strain rates the effect is more pronounced, as it seems that the contribution of the β-process is shifted to higher strain rates for the 'wet' samples. This shift is in accordance with the reduction in the glass transition temperature with an increase of the water content, as observed in the DMTA experiments (Fig. 1). Since the β-process is shifted to lower temperatures, the typical time-scale of this process will decrease and hence the onset of the β-contribution will shift to higher strain rates. The influence of an increase of the water content from 0.5 to 2.3 wt% could be modelled by changing the pre-exponential factors to: $C_{0,\alpha} = 10^{33}$ s^{-1} and $C_{0,\beta} = 10^{46}$ s^{-1}.

4. Conclusions

Dynamic mechanical thermal analysis of CARILON polymer of DP P1000 grade reveals the existence of three molecular relaxations. The α-process, which is assumed to be of crystalline nature, and the β- and γ-processes, related to the primary and secondary glass transition of the amorphous phase respectively. Over the range of temperatures and strain rates covered in this study, the tensile yield deformation behaviour of the DP P1000 material also gives

Table 1
Fit parameters according to Eq. (1), for 'dry' CARILON polymer of DP P1000 grade

CARILON DP P1000

Process	α	β
ΔH (kJ/mol)	352	262
v_i (nm^3)	4.6	2.0
$C_{0,i}$ (s^{-1})	5×10^{32}	1.5×10^{45}

evidence of the contributions of three stress- and temperature-activated deformation processes. The stress- and temperature dependences of the crystalline α-process and the amorphous β-process were determined in the assumption that both processes act in parallel. As contribution of the γ-process was only revealed at a temperature of −50°C, the available data was to limited to perform a similar analysis on this relaxation mechanism.

An increase in the water content from 0.5 to 2.3 wt%, in CARILON DP P1000, results in a selective shift in the characteristic temperature of the glass transition. Consequently, the occurrence of the yield behaviour related to the β-process is shifted to higher strain rates and/or lower temperatures.

References

[1] Brubaker MM. US Patent 2.495.286 (Du Pont), 1950.
[2] Brubaker MM, Coffman D, Hoehn HH. J Am Chem Soc 1952;74:1509.
[3] Sen A. Advances in polymer science, 73/74. Berlin: Springer Verlag, 1986.
[4] Drent E. European Patent 121.965 (Shell), 1984.
[5] Drent E, von Broekhoven JAM, Doyle MJ. J Organomet Chem 1991;417:235.
[6] Wakker A, Kormelink HG, Verbeke P. Kunststoffe 1995;85(8):1056.
[7] Danforth RL, Machado JM, Jordaan JCM. Proc Soc Plast Engng (ANTEC) 1995;5:2302.
[8] Weinkauf DH, Kinneberg PA, Ash C. Proc Soc Plast Engng (ANTEC) 1995;5:2297.
[9] Boyd RH. Polymer 1985;26(3):323.
[10] Boyd RH. Polymer 1985;26(8):1123.
[11] Ward IM. Mechanical properties of solid polymers, New York: Wiley, 1983.
[12] Roetling JA. Polymer 1966;1:303.
[13] Bauwens-Crowet C, Bauwens J-C, Homès G. J Mater Sci 1972;7:176.
[14] Roetling JA. Polymer 1965;6:311.
[15] Roetling JA. Polymer 1965;6:315.
[16] Bauwens-crowet C, Bauwens J-C, Homès G. J Polym Sci A-2 1969;7:735.
[17] Ree T, Eyring H. J Appl Phys 1955;26:793.